

Model Predictive Control for Optimal Energy Management of an Island Wind Storage Hybrid Power Plant

A. AGUILERA-GONZALEZ * R. LOPEZ-RODRIGUEZ *,**
I. VECHIU * S. BACHA **

* *Univ. Bordeaux, ESTIA Institute of Technology. Techn. Izarbel, 64210 Bidart, France (e-mail: a.aguilera-gonzalez@estia.fr).*

** *Univ. Grenoble Alpes, Grenoble Institute of Technology, 38031 Grenoble, Cedex 1, France*

Abstract: This paper presents a Model Predictive Control-based Energy Management System for compliance with the day-ahead power dispatching plan of a hybrid power plant connected to the Guadeloupe Island electrical grid. The hybrid power plant combines a wind farm and a Li-ION battery energy storage system. The proposed EMS handles several operation rules, in order to solve the optimization problem while considering the production forecasting data as well as the battery lifespan. A simulation study is implemented via PowerFactory and Matlab.

Keywords: Modeling and simulation of power systems, Control of renewable energy resources, Model predictive control, Smart grids.

1. INTRODUCTION

Dependence on fossil fuels imports is a major problem in island territories. Renewable energy resources such as sun and wind are playing a key role in terms of reduction of petroleum-based fuels reliance as they are free and abundant in those overseas locations. However, the fluctuations caused by their random behavior render the scheduling more difficult while increasing the system operational costs (Jin et al., 2019).

Due to the variability of wind speed, wind turbines (WT) have intermittent power output and, consequently, the difficulties grow to meet day-ahead generation schedules. These issues are amplified in the context of island grids as the French Archipelago of Guadeloupe, which should be managed to enhance grid efficiency without affecting stability and energy quality (Rodríguez et al., 2016).

Hybrid Power Plants (HPP) provide a solution to these issues by associating renewable energy sources (RES) with other technologies of generation or storage into one smart generation facility. The smartness of the hybrid systems lies in its Energy Management System (EMS), which allows power dispatching according to a generation plan, as well as the supply of ancillary services like frequency and voltage regulation.

Several EMSs based on control methods and data acquisition have been developed to operate those HPP (Luna et al., 2017; Bukar and Tan, 2019). More recently, Model Predictive Control (MPC) has received increasing attention because it can incorporate both forecasts and updated information to decide the future behavior of the system while handling constraints efficiently. MPC integrates the RES production forecasts in the optimization problem, either in terms of the expected generation or in terms

of the primary source, (wind speed, solar irradiance, etc) (Abdeltawab and Y.Mohamed, 2015; Zhang et al., 2019; Chen et al., 2020). However, there is still a large number of difficulties with regard to effective load management, economic dispatch, and especially its high dependency on the accuracy of expected forecast data.

In this paper, an EMS is proposed for an existing wind-battery storage HPP injecting power into the Guadeloupe island grid. Predictive control and optimization are combined to guarantee compliance with the day-ahead power dispatching plan while managing the storage system charge/discharge cycles efficiently, in order to accomplish the day-ahead power dispatch plan while considering the battery lifespan. To test the strategy, realistic simulation scenarios were considered with different forecasting errors to prove the ability of the proposed method to compensate them. The complete system was implemented in PowerFactory while the control algorithm is executed in MATLAB.

This paper is organized as follows: Section 2 presents a description of the Grid-connected hybrid power plant. Section 3 introduces the HPP PowerFactory model. In Section 4 the MPC strategy proposed is developed and finally in Section 5 the results are shown and discussed.

2. GRID-CONNECTED HYBRID POWER PLANT

The Guadeloupe archipelago relies heavily on thermal non-renewable sources (coal, diesel and combustion turbines) for electricity generation. In 2018, 71, 8% of the electricity consumed was provided by the combustion of fossil fuels (Belfort et al., 2019). The electrical grid of the Guadeloupe Islands has a 63kV high voltage transmission system, composed of two big loops of overhead lines (see Fig. 1). The loop covering Basse-Terre is interconnected at the Jarry Nord/Jarry Sud substation with Grande-Terre's

loop, which is composed of 14 nodes that correspond to HTB/HTA substations each comprising two 63/21 kV step down transformers connecting loads and, in most cases, also reactive compensation stations.

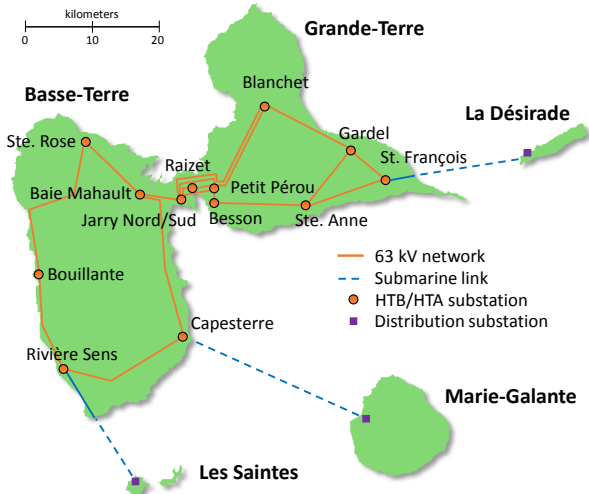


Fig. 1. Electrical substations on the Guadeloupe island.

This paper proposes a study to assess and validate the operation of a new hybrid wind/storage power plant at a particular point of the Guadeloupe electric grid (Sainte-Rose). The PowerFactory model of the Guadeloupe island electrical system shown in Fig. 2 was implemented from the data presented by Marin (2009). The shaded area corresponds to the point of common coupling (PCC) located within the node Sainte-Rose, where the HPP is connected.

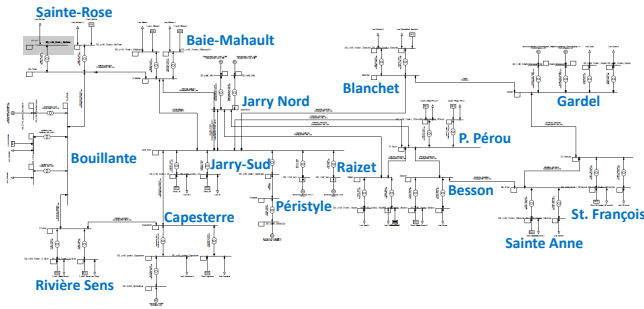


Fig. 2. Guadeloupe island electrical model.

3. SYSTEM MODELING

In this paper, a PowerFactory/Matlab co-simulation study was carried out in order to assess the impact of a wind-storage hybrid power plant, injecting power into one of the HTA busbars of the Sainte-Rose substation. The grid model was validated through simulation with respect to available data.

3.1 Wind generation system modeling

The wind generation system is depicted in Fig. 3. This system is composed of four 2MW induction generators containing the model of a DFIG (Doubly Fed Induction

Generators) wind turbines and converters. The transformers, busbars and underground lines used to rely the wind turbines to the PCC are also part of the system.

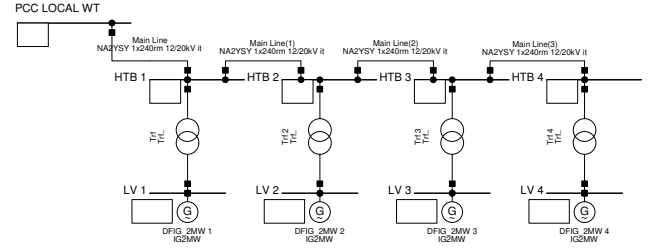


Fig. 3. Wind generation system model.

The WT model is based on the steady-state characteristics of the turbine presented by Rueda et al. (2014). Such model allows calculate the power extracted from the WT and considers electrical, mechanical, aerodynamic and control aspects.

3.2 Energy storage system modeling

The battery energy storage system (BESS) is based on the commercial storage solution Intensium Max 20M of Safe. For the project, four 1 MW 580 kWh Li-ion storage were considered. The modified Shepherd's model proposed by Tremblay and Dessaint (2009) was employed to describe the output voltage of a cell as a function of its capacity in ampere-hours (Ah). The battery cell terminal charge and discharge voltages are calculated as follows:

$$\begin{aligned} V_{ch} &= E_0 + R \cdot i^* - K \frac{Q_m}{i_t - 0.1Q_m} i^* - K \frac{Q_m}{Q_m - i_t} i_t + \Theta \\ V_{dch} &= E_0 + R \cdot i^* - K \frac{Q_m}{Q_m - i_t} i^* - K \frac{Q_m}{Q_m - i_t} i_t + \Theta \end{aligned} \quad (1)$$

where $\Theta = \bar{A} \cdot e^{\left(\frac{-\bar{B} \cdot i_t}{Q_{max}}\right)}$ is the term representing the exponential voltage. E_0 represents the battery constant voltage (V), R is the battery internal resistant (Ω), and K is the polarization constant (V/Ah). Meanwhile Q_m represents the maximum battery cell capacity (Ah), i^* is the filtered current, i_t is the dynamic current, \bar{A} is the exponential zone amplitude (V), and \bar{B} is the exponential zone time constant inverse (Ah^{-1}). In this work, to determine the parameters E_0 , R , \bar{A} , \bar{B} and K , an identification method from the manufacturing discharge curve was employed. This method applies optimization techniques to find the values of the X vector, subject to X^{min} and X^{max} as follows:

$$\begin{aligned} X &= [E_0 \ \bar{A} \ \bar{B} \ R \ K] \\ X^{min} &= [E_0^{min} \ \bar{A}^{min} \ \bar{B}^{min} \ R^{min} \ K^{min}] \\ X^{max} &= [E_0^{max} \ \bar{A}^{max} \ \bar{B}^{max} \ R^{max} \ K^{max}] \end{aligned} \quad (2)$$

to minimize the following cost function:

$$f_{obj}(X) = \sqrt{\sum_{i=1}^{i=n} \sum_{Q=0}^{Q=Q_{nom}} (V_{mes}(Q, I_i) - V(Q, I_i))^2} \quad (3)$$

where $I_i = I_1, \dots, I_n$ represents the discharge currents, which allows that the quadratic error among the manufacturer's voltage V_{mes} and the model estimations V , is minimized. For that, the amperes-hour delivered Q and the discharge current I are varied.

The four storage units comprising the BESS implemented in PowerFactory is shown in Fig. 4. It was also added the respective converters, two 2-winding transformers, one 3-winding, three busbars, and three underground lines.

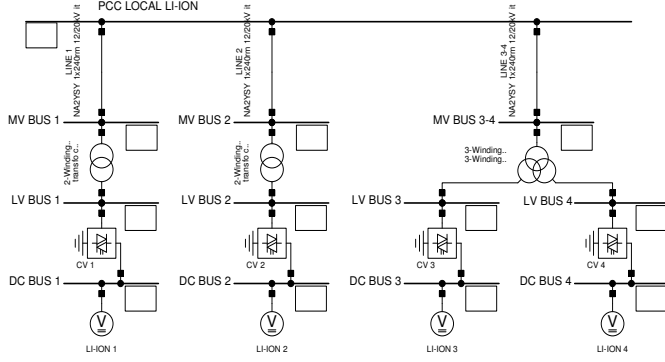


Fig. 4. Energy storage system model.

This model was validated through comparison with the battery model available on Simulink and presented in Aguilera-González et al. (2018). For this, a current input was imposed on both system representations (Matlab and PowerFactory) to observe the dynamic of battery states during the charging and discharging process.

4. MPC CONTROLLER

The EMS proposed warrants the continuous power injection from the HPP into the PCC, according to a commitment production profile determined from wind forecast data. For this, a control-oriented linear model of the BESS is required by the MPC controller to generate optimal control actions. The control scheme is presented in Fig. 5.

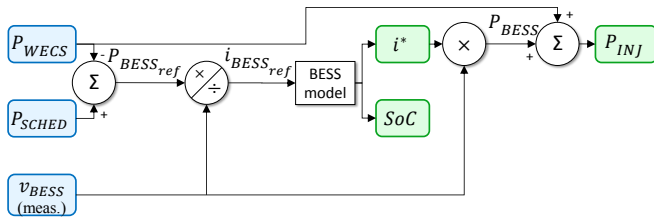


Fig. 5. HPP control scheme.

As can be seen, the power reference profile $P_{BESS_{ref}}$ is obtained from the commitment generation schedule P_{SCHED} and the output power of the wind energy system P_{WECS} , as:

$$P_{BESS_{ref}} = P_{SCHED} - P_{WECS} \quad (4)$$

where the signal P_{SCHED} represents the reference for the total power injected into the main grid. P_{INJ} is calculated as:

$$P_{INJ} = P_{WECS} + P_{BESS} \quad (5)$$

4.1 Storage System modeling for MPC

The proposed EMS uses predictive control to optimize the use of the storage system and thereby, the power injection into the utility grid. The prediction is based on the linear model of the storage system. With this purpose, the follow linear time-invariant (LTI) form is used:

$$\begin{aligned} x(k+1) &= Ax(k) + Bu(k) \\ y(k) &= Cx(k) \end{aligned} \quad (6)$$

where k represents the sampling time, $x(k) \in \mathbb{R}^n$ represents the system states, $u(k) \in \mathbb{R}^{n_u}$ the decision variable or input, and $y(k) \in \mathbb{R}^{n_r}$, the output controlled. Based on the discrete-time state-space representation obtained from Eq. (6), the BEES model is given by the next equations set:

$$\begin{aligned} i_t(k+1) &= i_t(k) + \Delta_t i_{BESS}(k) \\ i^*(k+1) &= (1 - \alpha) i^*(k) + \alpha i_{BESS}(k) \\ SOC(k+1) &= 100 \left(1 - \frac{i_t(k)}{Q} \right) - \left(\frac{\Delta_t i_{BESS}(k)}{Q} \right) \end{aligned} \quad (7)$$

where i_t is the dynamic current, i^* is the filtered current, SOC is the state-of-charge and Q is the battery capacity. i_{BESS} represents the battery current as the input system and α is the mitigating factor defined by:

$$\alpha = \frac{\Delta_t}{\tau + \Delta_t} \quad (8)$$

Δ_t represents the simulation step time and τ is the filter time constant. The model output vector containing the variables to optimize is given by:

$$y(k) = [i^*(k) \quad SOC(k)]^T \quad (9)$$

From the measured voltage v_{BESS} coming for the BESS (see Eq. (1)) and the filtered current i^* given by the model, the battery power can be computed as:

$$P_{BESS} = v_{BESS} \cdot i^* \quad (10)$$

where P_{BESS} is negative in case of charge (if $v_{BESS} = V_{ch}$) and positive in case of discharge (if $v_{BESS} = V_{dch}$).

4.2 MPC Algorithm

The EMS proposed combines an MPC controller with an optimization strategy based on the representation given by Eq (6). A multi-step ahead map is then required to apply the predictive methodology, which uses a state trajectory vector containing estimates for the next N_p sampling instants (i.e. the length of the optimization window is of N_p samples). This vector is described by:

$$\tilde{x}(k+1) = \begin{pmatrix} x(k+1) \\ \vdots \\ x(k+N_p) \end{pmatrix} \quad (11)$$

In the same way, the N_c elements conforming the future control sequence, (N_c is called the control horizon) are contained in the following vector:

$$\tilde{u}(k+1) = \begin{pmatrix} u(k) \\ \vdots \\ u(k+N_c-2) \\ u(k+N_c-1) \end{pmatrix} \quad (12)$$

where $\tilde{x}(k|\tilde{u}(k))$ denotes the fact that the state trajectory $\tilde{x}(k)$ calculation takes place at the current time step k and results from the control actions sequence $\tilde{u}(k)$ (Alamir, 2013). Applying the one-step-ahead prediction map, the instant $k+2$ is calculated as:

$$\begin{aligned} x(k+2) &= Ax(k+1) + Bu(k+1) \\ &= A[Ax(k) + Bu(k)] + Bu(k+1) \\ &= A^2x(k) + ABu(k) + Bu(k+1) \end{aligned} \quad (13)$$

For simplicity $N_p = N_c$ it is considered. Then, rewritten Eq. (13) in a more generally form, for any $i \in 1, \dots, N_p$, the state-space representation is given by:

$$x(k+i) = A^i x(k) + [A^{i-1}B, \dots, AB, B] \begin{pmatrix} u(k) \\ \vdots \\ u(k+i-2) \\ u(k+i-1) \end{pmatrix} \quad (14)$$

Then, it is possible to define a matrix $\Pi_i^{(n_u, N_p)}$ allowing the selection of the i^{th} vector of dimension n_u from the N_p elements of vector u (Alamir, 2013):

$$\begin{pmatrix} u(k) \\ \vdots \\ u(k+N_p-2) \\ u(k+N_p-1) \end{pmatrix} = \begin{pmatrix} \Pi_1^{(n_u, N_p)} \\ \vdots \\ \Pi_{i-1}^{(n_u, N_p)} \\ \Pi_i^{(n_u, N_p)} \end{pmatrix} \quad (15)$$

where each element of the $\Pi_i^{(n_u, N_p)}$ matrix is given by:

$$\Pi_i^{(n_u, N_p)} = (\mathbb{I}_{n_u i} \quad \mathbb{O}_{n_u i \times (N_p - i n_u)}) \quad (16)$$

so, the Eq. (14) can then be rewritten as:

$$x(k+i) = A^i x(k) + ([A^{i-1}B, \dots, AB, B] \cdot \Pi_i^{(n_u, N_p)}) \tilde{u}(k) \quad (17)$$

and the prediction of future states can be written in a compact form as:

$$x(k+i) = \Phi_i x(k) + (\Psi_i \cdot \Pi_i^{(n_u, N_p)}) \tilde{u}(k) \quad (18)$$

where $\Phi_i = A^i$ and $\Psi_i = [A^{i-1}B, \dots, AB, B] \cdot \Pi_i^{(n_u, N_p)}$ are constant matrices depending on state and input matrices, A and B respectively.

4.3 Power dispatch optimization

The aim of the EMS is ensuring that the power supplied to the main grid respect the operating rules while maximizing the plant's income. The disrespect of the injection band leads to penalties reducing the power plant profits. The power injections with excursions of 60 consecutive seconds

outside the limits are penalized with non-payment of the power supplied to the grid for the next 10 minutes. The plant revenue (PR) is a key indicator performance (KPI), which was established for monitoring the HPP profits. During the operation time, it can be calculated considering the energy selling price (SP in /c per kWh) as:

$$PR = \sum_{t=0}^{sim.time} P_{INJ}(t) \cdot SP(t) \cdot \partial(t) \quad (19)$$

where $\partial(t) = \begin{cases} 0 & \text{when a penalty condition is active} \\ 1 & \text{in other cases} \end{cases}$

The optimization objectives and the constraints to which the cost function is subject are explained in the following paragraphs:

Objectives

- **Power injection band respect:** A tolerance region (injection band) is established on the basis of the injection schedule. This objective consists in minimizing the difference among P_{INJ} and P_{SCHEd} , which is equivalent to attracting P_{INJ} towards the center of the tolerance region (see Fig. 6).

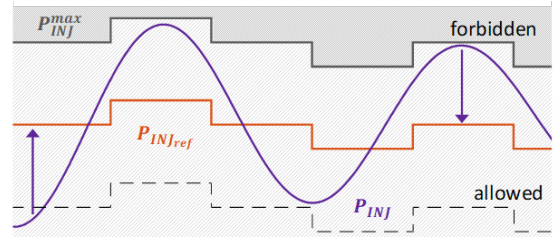


Fig. 6. Power injection band.

The upper and lower bounds are given by:

$$\begin{aligned} P_{uplim} &= P_{SCHEd} + 0.25 \cdot P_{MAX} \\ P_{lowlim} &= P_{SCHEd} - 0.25 \cdot P_{MAX} \end{aligned} \quad (20)$$

where P_{MAX} is the plant generation capacity (8MW).

- **State-of-charge maximization:** This objective consists in minimizing the difference among the current SOC and reference established at 90%.

Constraints

- **Maximal power injection:** When the wind-generated power is close to maximal of the WP capacity and the BESS is being discharged, P_{INJ}^{max} is fixed as follow:

$$P_{INJ}^{max} = P_{SCHEd} + tol \cdot P_{MAX} \quad (21)$$

conversely, its minimum value is zero when the WT is not generating and the BESS is not being discharged. In order to avoid penalties, rather than setting constraints on the injection band limits, the constraint P_{INJ}^{max} is placed on the band ceiling as:

$$P_{INJ} \leq P_{INJ}^{max} \quad (22)$$

In this way, instead of allowing injections greater than the upper limit, extra available power can be used to charge the BESS. This constraint was defined through the current i^* , which is a controlled output.

- *Rate of change of power injected:* the rate of change limits of the power injected were defined by the objectives. This can be put in inequality form, giving:

$$\begin{aligned} \frac{P_{MAX}}{300} MW/s \leq \frac{dP_{INJ}}{dt} \leq \frac{P_{MAX}}{30} MW/s \quad (23) \\ -\frac{P_{MAX}}{600} MW/s \leq \frac{dP_{INJ}}{dt} \leq \frac{-P_{MAX}}{60} MW/s \end{aligned}$$

which are constraints for upward and downward steps of dP_{INJ}/dt . In other words, these constraints limit the rate of change of P_{INJ} so as to avoid big changes in the power transferred towards the grid.

- *State-of-charge:* The BESS must be operated respecting the recommendations of the manufacturer in terms of depth-of-discharge and charging rates as to avoid its replacement before 15 years. To achieve this, a SOC operation region is established as follows:

$$20\% \leq SOC \leq 80\% \quad (24)$$

- *BESS maximum charge current:* The maximum continuous charge and discharge currents (respectively 3280A and $-6400A$) are defined for the BESS. Hence, the battery current is constrained as:

$$-6400 \leq i^* \leq 3280 \quad (25)$$

4.4 Prediction and optimization strategy

The aim of the optimization strategy is that of generating a control signal that optimizes a cost function over the prediction horizon. The following quadratic cost function is then defined:

$$\begin{aligned} \Gamma(k) = \sum_{i=1}^{N_p} \left\{ \lambda_1 \|P_{INJ} - P_{INJref}\|^2 + \right. \quad (26) \\ \left. \lambda_2 \|SOC - SOC_{ref}\|^2 + \left[\Pi_i^{(nu, N_p)} \tilde{u} \right]^T Q_u \left[\Pi_i^{(nu, N_p)} \tilde{u} \right] \right\} \end{aligned}$$

where the control objectives are expressed in a quadratic form. λ_1 and λ_2 are weights allowing to increase/decrease the importance of an objective with respect to the other. \tilde{u} is the vector containing the N_p elements conforming the control sequence going from $u(k)$ to $u(k + N_p - 1)$. $Q_u \in \mathbb{R}^{n_u \times n_u}$ is a symmetric positive definite matrix for weighting and adjusting the control effort of the inputs, and $\Pi_i^{(nu, N_p)}$ is an identity matrix concatenated with a zero matrix whose sizes change with i , i.e.:

$$\Pi_i^{nu, N_p} = \left(\mathbb{I}_{n_u i \times n_u i} \quad \mathbb{0}_{n_u i \times (N_p - 1) n_u} \right) \quad (27)$$

Here, Γ can be interpreted as the cost obtained by the evaluation of the future control actions function \tilde{u} using the future references P_{INJref} and SOC_{ref} and the present system state $x(k)$ within the time horizon $[k, k + N_p]$.

An appropriate optimization algorithm is used to reduce future errors based on such a quadratic function and in the presence of linear constraints Alamir (2013). The MPC prediction algorithm is defined based on the BESS model to feed the cost function at every time step (see Aguilera-González et al. (2018)).

5. RESULTS

To test the robustness of our strategy, a 24h profile of wind power production from Guadeloupe Island was analyzed. Two scenarios representing 3-hours commitment profiles were chosen (as can be seen in Fig. 7). These results deal with the electrical grid of Guadeloupe as well as the HPP modeled under PowerFactory environment, while the MPC and the optimization strategy was executed in Matlab.

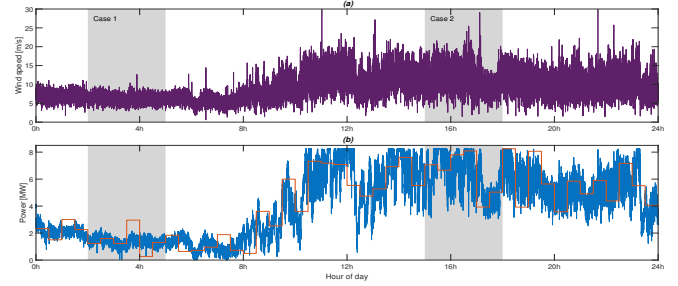
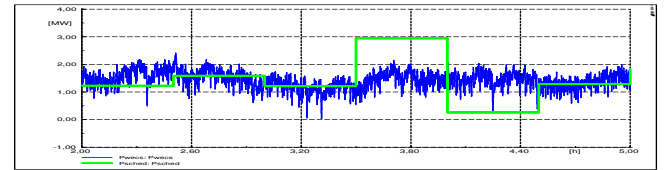
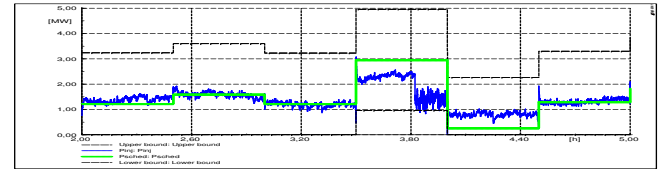


Fig. 7. Wind and power profiles during 24h.

- *Case 1:* In Fig. 8 a 3-hours commitment profile with steps of 30 minutes is shown, a prediction horizon (N_p) of 15 seconds was defined. In this first case, greater importance was given to respect of the injection band over the SOC maximization.



(a) Wind production and the day-ahead dispatch power profiles.



(b) Power injection band.

Fig. 8. Profile and Injection band at morning (2h-5h).

Fig. 8b shows that the injected power P_{INJ} stays inside the tolerance region of 2 MW above and below of the commitment profile, (P_{SCHED}). Between $t = 3.5$ hours and $t = 3.8$ hours the power transferred to the grid is less than the commitment. This is because the WECS output smaller than expected that caused the storage system to discharge from its initial SOC of 30 % until reaching 20 % (the lower SOC level allowed), as depicted in Fig. 9.

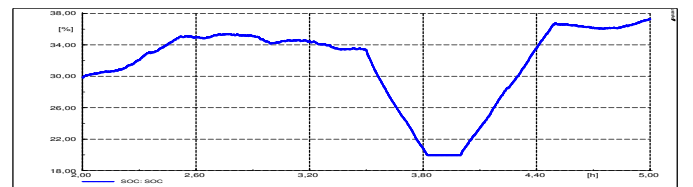
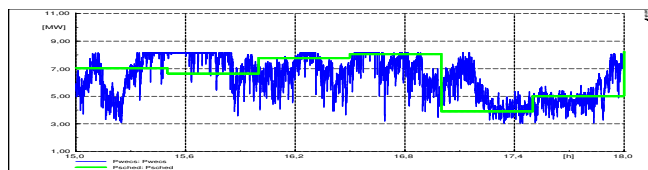
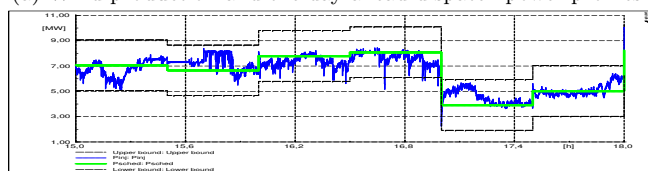


Fig. 9. Battery SOC in case 1.

- *Case 2:* In Fig. 10 a second 3-hours commitment profile at afternoon is shown. In this case, more importance was given to the objective of the SOC maximization. Initial SOC was fixed at 78%.



(a) Wind production and the day-ahead dispatch power profiles.



(b) Power injection band.

Fig. 10. Profile and Injection band at afternoon (15h-18h).

In this second case, the Fig. 10b shows that the injected power P_{INJ} is greater than commitment (WECS overproduction between 15.5-16 hours), but this injection stays always inside the tolerance region. During this time, the wind being stronger than expected makes to charge the battery until the upper limit, 80% SOC (Fig. 11). As shown, the proposed controller is able to efficiently manage the BESS with respect to the constraints defined.

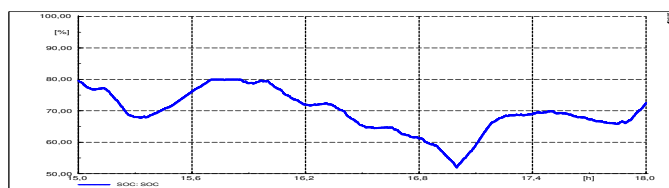


Fig. 11. Battery SOC in case 2.

6. CONCLUSION

In this work, an energy management strategy for the power dispatch of a wind-BESS HPP injecting power into the electrical grid of Guadeloupe Island is proposed. For that, a model predictive control and optimization strategy were developed to drive the storage system with respect to two optimization objectives: respect of a defined region for the power injection, and maximization of the storage system SOC. The strategy uses the model of the BESS to find optimal solutions that bring the system's predicted output close to a trajectory of future power injections defined.

The controller performance was verified in co-simulation PowerFactory/Matlab using real wind speed data collected in Guadeloupe Island. The methodology proved its ability to efficiently manage the power output of the hybrid power plant and meet generation schedules with respect to the constraints defined. The prediction algorithm developed here is compatible with a quadratic programming solver tool to minimize a cost function subject to a set of linear constraints. Those constraints represent the physical and operational burdens of the hybrid plant studied. In future work, forecast reliability analysis for the implementation of the MPC control strategy should be considered.

7. ACKNOWLEDGMENT

The authors gratefully acknowledge the financial support of the Aquitaine region and BPI France in the context of InsulGrid project.

REFERENCES

- Abdeltawab, H. and Y.Mohamed (2015). Market-oriented energy management of a hybrid wind-battery energy storage system via mpc with constraint optimizer. *IEEE Trans. on Industrial Electronics*, 62(11), 6658–6670.
- Aguilera-González, A., Vechiu, I., López, R., and Bacha, S. (2018). Mpc ems for a grid-connected renewable energy/battery hybrid power plant. In *7th Int. Conf. on Renewable Energy Research and Apps (ICRERA 2018)*, 738–743. Paris, France.
- Alamir, M. (2013). *A Pragmatic Story of Model Predictive Control: Self-Contained Algorithms and Case-Studies*. CreateSpace Independent Publishing Platform.
- Belfort, A., OREC, and Synergile (2019). Les chiffres clés de l'énergie en guadeloupe. bilan 2018. Report, Observatoire régional de l'énergie et du climat de la Guadeloupe. Comité de l'observatoire régional de l'énergie et du climat (ADEME, Région Guadeloupe, DEAL, EDF, Météo-France, SYMEG, SARA et Synergile).
- Bukar, A. and Tan, C. (2019). A review on stand-alone photovoltaic-wind energy system with fuel cell: System optimization and energy management strategy. *Journal of Cleaner Production*, 221, 73 – 88.
- Chen, Y., Deng, C., Li, D., and Chen, M. (2020). Quantifying cumulative effects of stochastic forecast errors of renewable energy generation on energy storage soc and application of hybrid-mpc approach to microgrid. *Int. Journal of Electrical Power & Energy Systems*, 117.
- Jin, H., Liu, P., and Li, Z. (2019). Dynamic modeling and design of a hybrid compressed air energy storage and wind turbine system for wind power fluctuation reduction. *Computers & Chemical Eng.*, 122, 59 – 65.
- Luna, A., Díaz, N., Graells, M., Vásquez, J., and Guerrero, J. (2017). Mixed-integer-linear-programming-based ems for hybrid PV-wind-battery microgrids: Modeling, design, and experimental verification. *IEEE Trans. on Power Electronics*, 32(4), 2769–2783.
- Marin, D. (2009). *Study of wind power integration in the island grids*. Theses, Ecole Centrale de Lille. URL <https://tel.archives-ouvertes.fr/tel-00577097>.
- Rodríguez, E., Osório, G., Godina, R., Bizuayehu, A., Lujano, J., and Catalão, J. (2016). Grid code reinforcements for deeper renewable generation in insular energy systems. *Renewable and Sustainable Energy Reviews*, 53, 163 – 177.
- Rueda, J., Korai, A., Cepeda, J., Erlich, I., and Gonzalez-Longatt, F. (2014). *Implementation of Simplified Models of DFIG-Based Wind Turbines for RMS-Type Simulation in DIgSILENT PowerFactory*, chapter 9, 197–220. Springer International Publishing, Cham.
- Tremblay, O. and Dessaint, L. (2009). Experimental validation of a battery dynamic model for ev applications. *World Electric Vehicle Journal*, 3, 289–298.
- Zhang, Y., Meng, F., Wang, R., Kazemtabrizi, B., and Shi, J. (2019). Uncertainty-resistant stochastic mpc approach for optimal operation of chp microgrid. *Energy*, 179, 1265 – 1278.